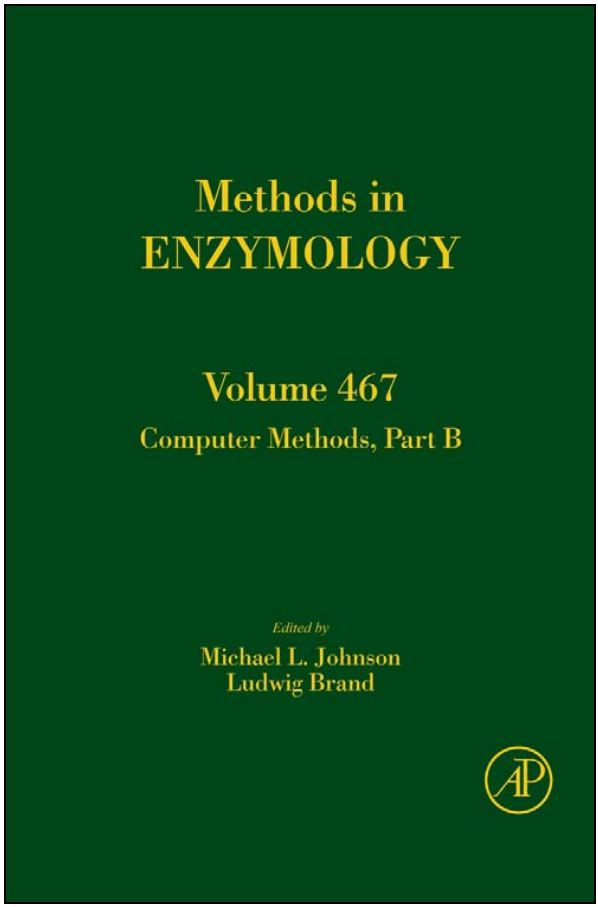

From: Maurizio Tomaiuolo, Joel Tabak, and Richard Bertram, Correlation Analysis: A Tool for Comparing Relaxation-Type Models to Experimental Data. In Michael L. Johnson and Ludwig Brand, editors: Methods in Enzymology, Vol. 467, Burlington: Academic Press, 2009, pp. 1-22.
ISBN: 978-0-12-375023-5

CHAPTER ONE

Correlation Analysis: A Tool for Comparing Relaxation-Type Models to Experimental Data

Maurizio Tomaiuolo,* Joel Tabak,* *and* Richard Bertram†

Contents

Abstract

We describe a new technique for comparing mathematical models to the biological systems that are described. This technique is appropriate for systems that produce relaxation oscillations or bursting oscillations, and takes advantage of noise that is inherent to all biological systems. Both types of oscillations are composed of active phases of activity followed by silent phases, repeating periodically. The presence of noise adds variability to the durations of the different phases. The central idea of the technique is that the active phase duration may be correlated with either/both the previous or next silent phase duration, and the resulting correlation pattern provides information about the dynamic structure of the system. Correlation patterns can easily be determined by making scatter plots and applying correlation analysis to the cluster of data points. This could be done both with experimental data and with model simulation data. If the model correlation pattern is in general agreement with the experimental data, then this adds support for the validity of the model.

* Department of Biological Science and Program in Neuroscience, Florida State University, Tallahassee, Florida, USA
† Department of Mathematics and Programs in Neuroscience and Molecular Biophysics, Florida State University, Tallahassee, Florida, USA

Methods in Enzymology, Volume 467
ISSN 0076-6879, DOI: 10.1016/S0076-6879(09)67001-4

Otherwise, the model must be corrected. While this tool is only one test of many required to validate a mathematical model, it is easy to implement and is noninvasive.

1. Introduction

Multivariable systems in which one or more of the variables change slowly compared with the others have the potential to produce relaxation oscillations. These oscillations are characterized by a ''silent state'' in which the fast variables are at a low value, and an ''active state'' in which the fast variables are at a high or stimulated value. The fast variables jump back and forth between these states as the slow variables slowly increase and decrease. The fast variable time course thus resembles a square wave, while the slow variable time course has a saw-tooth pattern. The van der Pol oscillator is a classic example for this system (van der Pol and van der Mark, 1928). Several important biological and biochemical systems have the features of relaxation oscillators, including cardiac and neuronal action potentials (Bertram and Sherman, 2005; van der Pol and van der Mark, 1928), population bursts in neuronal networks (Tabak *et al.*, 2001), the cell cycle (Tyson, 1991), glycolytic oscillations (Goldbeter and Lefever, 1972), and the Belousov–Zhabotinskii chemical reaction (see Murray, 1989, for discussion). Bursting oscillations are a generalization of relaxation oscillations, where the active state is itself oscillatory (Bertram and Sherman, 2005; Rinzel and Ermentrout, 1998). Thus, bursting consists of fast oscillations clustered into slower episodes. These oscillations are common in nerve cells (see Coombes and Bressloff, 2005, for many examples) and hormone-secreting endocrine cells (Bertram and Sherman, 2005; Dean and Mathews, 1970; Li *et al.*, 1997; Tsaneva-Atanasova *et al.*, 2007; Van Goor *et al.*, 2001).

Analysis techniques for models of relaxation-type oscillations are well developed. For pure relaxation oscillations a phase-plane analysis is typically used (Strogatz, 1994). For bursting oscillations, a geometric singular perturbation analysis, often called fast/slow analysis, is the standard analytical tool (Bertram *et al.*, 1995; Rinzel, 1987; Rinzel and Ermentrout, 1998). From these analyses one can understand features such as threshold behaviors, the effects of perturbations, the conversion of the system from an oscillatory to a stationary state or *vice versa*, the slowdown of the fast oscillations near the end of the active state that is often observed during bursting, or the subthreshold oscillations that are sometimes observed during the silent phase of a burst. Thus, the analysis is useful for understanding the dynamic behaviors observed experimentally.

While most of the analysis described above assumes that the system is deterministic, in reality all of the biological and biochemical systems on

which the models are based contain noise. The noise could be due to intrinsic factors such as a small number of substrate molecules or ion channels of a certain type. It could also be due to extrinsic factors such as stochastic synaptic input to a neuron, stochastic activation of G-protein-coupled receptors by extracellular ligands, or measurement error. Whatever the origin, noise can make it more difficult to detect some subtle features of the oscillation. This makes it harder to know how well the mathematical model reproduces the behavior of the system under investigation, since key model predictions may depend on the detection of these subtle features in the experimental record (Bertram *et al.*, 1995).

In this chapter, we describe a tool based on statistical correlation analysis that can be used to compare the behavior of a mathematical model against experimental data and thus help to determine the validity of the model. This method is designed for relaxation-type models and makes use of intrinsic noise in the system. Subtle features such as spike frequency slowdown or subthreshold oscillations are not utilized. Instead, we look at correlation patterns between the durations of active and silent phases in the experimental data, and in simulation data generated by stochastic implementations of the corresponding model. We demonstrate the use of the tool through four examples. First, we show how it can be (and has been) used to make a powerful (and testable) prediction that can distinguish the type of slow negative feedback underlying a relaxation oscillation. Second, we demonstrate how the tool can be used to study bursting oscillations, focusing on the "square wave" class of bursters. The third example focuses on "elliptic bursters," and demonstrates that the correlation pattern can distinguish one type of bursting from another. Finally, we apply the correlation analysis to a model of the pituitary lactotroph, a cell in the pituitary gland that secretes the hormone prolactin. We contrast the correlation patterns obtained with this model with experimental electrical data from a pituitary lactotroph cell line.

2. Scatter Plots and Correlation Analysis

In a deterministic system, the duration of each active phase of a relaxation-type oscillator is the same, and the duration of each silent phase is the same. However, when the system exhibits random fluctuations, or noise, durations will vary since the noise can perturb the system prematurely from one state to another. We measure the duration of each silent phase and each active phase (see Appendix for the algorithm used for bursting oscillations), and then make a scatter plot of the active phase durations versus the previous silent phase durations. A separate scatter plot is made of the active phase durations versus the following silent phase durations. We then use

these scatter plots to look for correlations between the active phase and silent phase durations. This can be done using simulation data from a model, or using actual data for the corresponding experimental system. As we demonstrate in the examples below, one expects certain correlation patterns to exist, based on the dynamic structure of the model. The validity of the model is supported (but not established) if the expected correlation patterns match those from the experimental data. If there is no match, then it is likely that the model should be modified or the parameters adjusted. This approach can be used for relaxation oscillations or bursting oscillations, and is most useful when there are enough experimental data to establish statistical confidence in the correlation patterns.

3. Example 1: Relaxation Oscillations

We consider a system whose activity a is controlled by a fast positive feedback and a slow negative feedback process. This forms the basis for many biological oscillators (Ermentrout and Chow, 2002; Friesen and Block, 1984; Tsai *et al.*, 2008). The activity varies according to:

$$\tau_a \frac{da}{dt} = -a + a_\infty(wa - \theta_0) + i. \tag{1.1}$$

This equation means that a tends to reach a steady state determined by the steady-state input/output function (or activation function) a_∞, with a time constant τ_a (which is set to 1, so time is relative to τ_a). The function a_∞ is a sigmoid function of its input (Fig. 1.1) which is proportional to the system's output, a. This injection of the activity back into the system's input represents positive feedback and the gain of the feedback loop is set by the parameter w. The other parameter, θ_0, represents the half-activation input: if the input is below θ_0, the output (activity) will be low, and if the input is above θ_0, then the output will be high. Finally, the term i provides for a possible external input to the system, such as a brief resetting perturbation.

This activity equation can describe, for example, the mean firing rate within a network of neurons connected by excitatory synapses (Tabak *et al.*, 2000, 2006; Wilson and Cowan, 1972). In this mean field framework, the network steady-state input/output function a_∞ depends on the input/output properties of the single cells, the degree of heterogeneity in the network, as well as the synaptic dynamics. The parameter w represents the degree of connectivity in the network while θ_0 sets the amount of excitation that neurons need to receive to become activated.

Such a system will always evolve to a steady state (defined by $da/dt = 0$). For some parameter values, the system may have two stable steady states, one at a high- and one at a low-activity level. This is a direct consequence of the

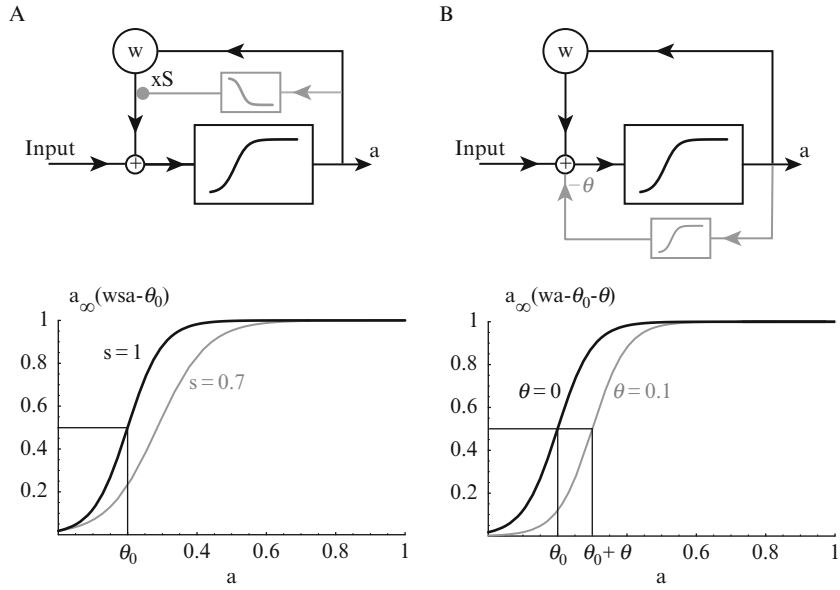

Figure 1.1 System with (fast) positive feedback and two types of (slow) negative feedback. The positive feedback loop is shown in black; the negative feedback loop is in gray. (A) System with divisive feedback, which decreases the gain of the positive feedback loop by a factor s (upper panel). The effect of this feedback is a decrease of the slope of the system steady-state activation. (B) System with subtractive feedback, which decreases the effective input by θ (upper panel). The effect of this feedback is a shift of the steady-state activation function of the system to the right. In both cases, the steady-state output function is given by $a_\infty(x) = 1/(1 + \exp(-x/k_a))$.

positive feedback. To create relaxation oscillations, we add a slow negative feedback process. This will allow the system to switch repetitively between the high and low steady states. We consider two types of slow negative feedback.

The first type is *divisive feedback*. This feedback reduces the amount of positive feedback and is implemented using a slow variable, s, according to:

$$\tau_a \frac{da}{dt} = -a + a_\infty(wsa - \theta_0) + i, \tag{1.2}$$

$$\tau_s \frac{ds}{dt} = -s + s_\infty(a), \tag{1.3}$$

where s_∞ is a decreasing function of a, so that s decreases during high activity episodes and recovers when the activity is low. Figure 1.1A illustrates that such divisive feedback decreases the slope of the input/output relationship of the system. In a mean field neuronal network model, for example, synaptic depression would be implemented as divisive feedback (Shpiro *et al.*, 2007; Tabak *et al.*, 2006).

The second type is *subtractive feedback*. In this case, the half-activation point of the system is shifted by a slow variable, θ, according to:

$$\tau_a \frac{da}{dt} = -a + a_\infty(wa - \theta_0 - \theta) + i, \tag{1.4}$$

$$\tau_\theta \frac{d\theta}{dt} = -\theta + \theta_\infty(a), \tag{1.5}$$

where, θ_∞ is an increasing function of a, so that θ increases during high activity and decreases during low activity. Figure 1.1B shows how subtractive feedback shifts the activation function to the right, so more input is necessary to achieve a given output. In a mean field neuronal model, adaptation of cell excitability by outward ionic currents would be implemented as subtractive feedback (Shpiro *et al.*, 2007; Tabak *et al.*, 2006).

Both the models defined by Eqs. (1.2) and (1.3) (s-model) and by Eqs. (1.4) and (1.5) (θ-model) generate relaxation oscillations. We first examine the oscillations generated by the s-model (Fig. 1.2A). The upper panel shows the time courses of a and s. Activity is oscillating between active (high a) and silent (low a) phases. During the silent phase (1), s increases, increasing the level of positive feedback, until activity jumps to a high level (2). This starts the active phase (3), during which s decreases, decreasing the level of positive feedback. When s is low enough, there is not enough positive feedback to sustain the high activity, a falls to the low level (4) and the cycle repeats.

We can gain qualitative understanding of this cyclic activity by using a "phase-plane" representation. Instead of plotting time courses, we plot $a(t)$ versus $s(t)$ in the (a, s) plane (Fig. 1.2A, lower panel). First, we use the fact that s is much slower than a, and, for each value of s, now treated as a parameter, plot the steady states of Eq. (1.2) (the points for which $da/dt = 0$). We obtain an S-shaped curve, called the a-nullcline. For some values of s there are three possible steady states, one low (stable), one high (stable), and one intermediate that is unstable. Thus, within that range of s values the system is bistable, as mentioned above, with the middle state acting as a threshold: at any given time, if a is below this threshold it will fall to the low steady state; if it is above threshold it will rise to the high steady state.

We now allow s to vary and plot the state of the system, represented by a trajectory in the (a, s) plane. Assume a is low initially, so we start on the lower branch of the S-curve. In this case s increases slowly according to Eq. (1.3) and the trajectory follows the lower branch (1). This continues until s passes the value where the low and middle steady states meet (the low "knee" of the a-nullcline, LK), so there is no other steady state of Eq. (1.2) other than the upper steady state. Thus, the system jumps to the high activity state (2). Once in the high activity state, s decreases and the system slowly tracks the high branch of the S-curve, moving to the left; this is the active phase (3). Eventually, the trajectory passes the high knee (HK) of the

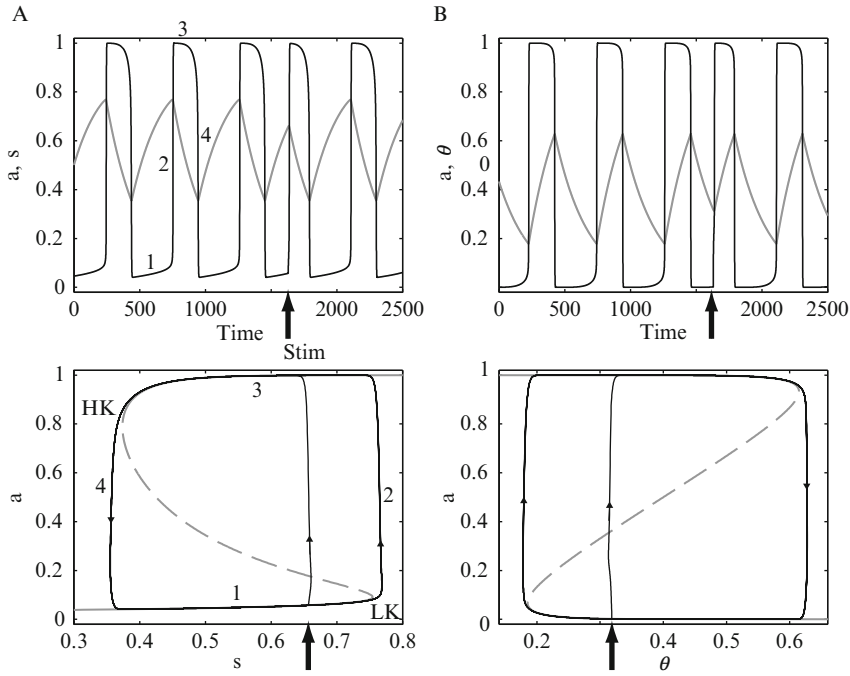

Figure 1.2 The s-model and the θ-model produce relaxation oscillations with similar properties. (A) The s-model. Upper panel, oscillatory time courses of s and a. A brief stimulation ("stim," arrow) before full recovery triggers an active phase of shorter duration than the unstimulated ones. Lower panel, the oscillations are represented by a trajectory in the (a, s) plane that slowly tracks the lower and upper branches of the a-nullcline (S-shaped curve) and quickly jumps between the branches at the transition points, or knees of the S-curve. LK, low knee; HK, high knee; stim, stimulation that provokes a premature active phase. (B) The θ-model. Upper panel, time courses of θ and a. Lower panel, phase-plane trajectory superimposed on the Z-shaped a-nullcline.

S-curve (HK) where the upper steady state meets the middle steady state. Activity then falls abruptly to the low level (4) and the cycle repeats. In the phase plane, the effect of a brief stimulation (arrow in Fig. 1.2A) is apparent: if the stimulus (i) is large enough to bring a above the middle branch of the S-curve (i.e., the threshold), a will immediately jump up to the high state. The resulting premature active phase will be shorter than an unstimulated active phase because it starts at a lower value of s, so less time will be needed to reach the HK. Note that an active phase can also be prematurely terminated by a stimulation that brings a below the threshold. In that case, the following silent phase will also be correspondingly shorter (not shown).

Figure 1.2B shows that the θ-model also generates relaxation oscillations and responds to brief perturbations in a very similar way. The only visible difference is that the a-nullcline is a Z-shaped curve instead of S-shaped. This is because θ increases with high activity and decreases during periods of low activity, in an opposite fashion to s. In both models, the oscillations of the slow variable allow the system to switch between the active and silent phases. The system tracks the stable branches of the a-nullcline until it reaches a knee, where it transitions from one branch to the other.

In many cases, only the activity variable a, but not the feedback variables s or θ, would be readily measurable in experiments. The two models generate oscillations in a with the same properties, so how can one tell whether experimentally observed relaxation oscillations are controlled by a divisive or a subtractive feedback mechanism? In the following, we show that noise that is intrinsic to the biological system has different effects on the two models, so one would only need to record spontaneous oscillations to distinguish between the two possible models.

We include noise by replacing i in Eq. (1.4) with $m\eta$, where m is the magnitude of the noise and η is a normally distributed random variable. Results presented in the following are not overly sensitive to the way noise is added to the activity. The most important assumption is that noise perturbs the system's activity, not the slow feedback process.

The simulations with noise produce episodic activity as shown in Fig. 1.2, but with variable durations of the active and silent phases. The activity time course is shown in Fig. 1.3A for the s-model with noise. We expect that noise induces early (or delayed) transitions between the silent and active phases, leading to shortened (or lengthened) active and silent phases. To evaluate these effects, we plot active phase duration as a function of the *preceding* silent phase (Fig. 1.3B) or *following* silent phase (Fig. 1.3C). We observe a strong positive correlation between the length of the active phase and preceding—but not following—silent phase. This correlation pattern (Fig. 1.3B and C) is the signature of relaxation oscillations that rely on slow divisive feedback.

The cause for this pattern can be deduced from Fig. 1.3A. Transitions between silent to active phases can occur at very different levels of the slow variable s, but the transitions from active to silent phases seem to occur around the same value of s with very little change from period to period. This implies that a shorter silent phase corresponds to a lower value of s at active phase onset, and thus to a correspondingly shorter active phase duration (cf. Fig. 1.2A). The correlation shown in Fig. 1.3B therefore illustrates that all the variability in active phase duration is due to variability in the preceding silent phase duration. On the other hand, regardless of active phase duration, the following silent phase starts at the same s value as all other silent phases and therefore is not influenced by active phase duration. Thus, there is no correlation between active phase and following silent phase duration

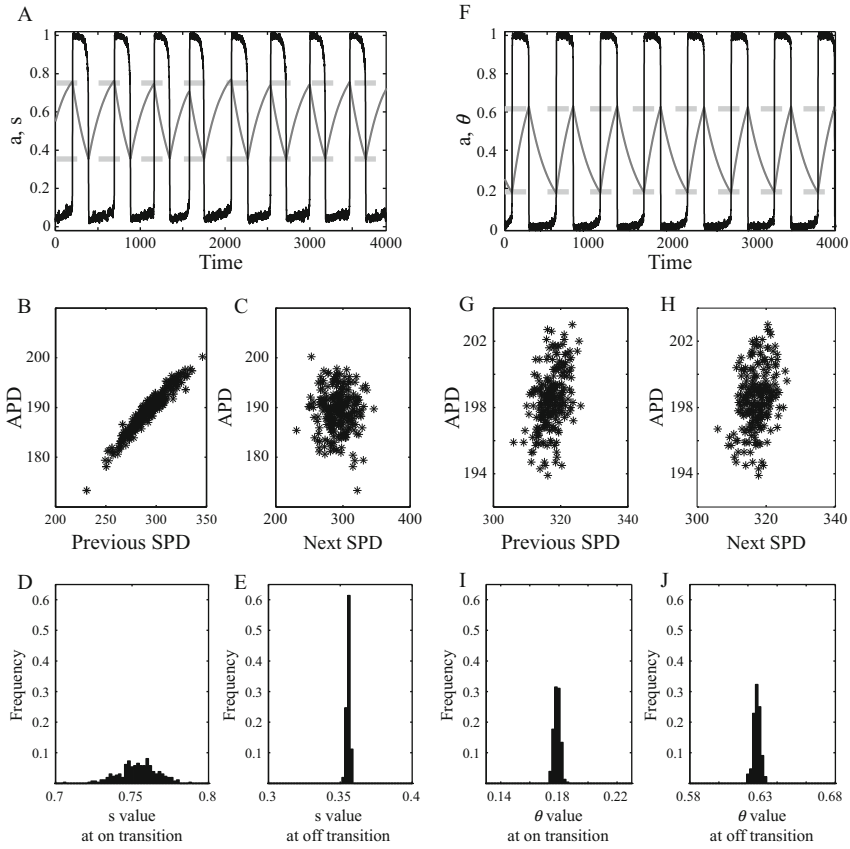

Figure 1.3 Activity patterns generated by the two types of relaxation oscillators. (A) Time courses of a and s generated by the s-model with noise. There is visibly more variability of the s value at the on transition than at the off transition (mean values at the transitions are indicated by the horizontal-dashed lines). A strong correlation between active phase and preceding (B), but not following (C), silent phase duration corresponds to a wide distribution of s at the on transition (D) and a narrow distribution of s at the off transition (E). (F) Time courses of a and θ generated by the θ-model with noise. There is a weak correlation between active phase duration and both the preceding (G) and following (H) silent phase duration. They correspond to equal amounts of variability in the distributions of θ at the on (I) and off (J) transitions. APD, active phase duration; SPD, silent phase duration.

(Fig. 1.3C), that is, the variability in active phase duration does not cause any of the variability in the following silent phase duration.

To illustrate this discrepancy between the "on" (silent to active) and the "off" (active to silent) transitions, we plot histograms of the value of s at the transitions. Figure 1.3D shows the wide distribution of s values at the "on"

transition, while Fig. 1.3E reveals a very narrow distribution of s values at the off transition. Thus, the correlation pattern shown in Fig. 1.3B and C is due to the large variations of s at the on transition relative to the off transition. Note that if the variability of s at the off transition was greater, then the correlation between active and preceding silent phase duration would be reduced, since there would be some variability in active phase duration not caused by variability in the length of the silent phase. Also, with less variability at the on transition, the small amount of variability at the off transition would have a larger impact and there would be a tendency for a longer active phase to be followed by a longer silent phase. If the variability of s values at both the on and off transitions was equal, we would observe a weak (but significant) correlation between active phase duration and *both* preceding and following silent phase durations. This situation occurs with the θ-model.

Figure 1.3F shows time courses generated by the θ-model with noise. For the same amount of noise as used in the s-model, there is less variability in the length of active and silent phases. More importantly, the variability of θ is similar at the on and off transitions (Fig. 1.3I and J). This results in weak but significant correlation between the duration of the active phase and both preceding (Fig. 1.3G) and following (Fig. 1.3H) silent phases. Thus, if the correlation pattern is similar to Fig. 1.3B and C then divisive feedback is likely involved, while if the correlation pattern is similar to Fig. 1.3G and H a subtractive feedback is involved.

We now give a qualitative explanation for the differences in the amount of variability of the slow negative feedback variables at the on and off transitions, since these differences cause the differences in the correlation patterns. It is possible to predict the correlation patterns using survival analysis of particles in a two-well potential (Lim and Rinzel, submitted). Here, we give an equivalent but more intuitive explanation based on geometrical arguments. Again, we use the difference of time scales between the fast activity and the slow negative feedback processes, and we begin with the s-model (divisive feedback).

There are two contributing factors to the observed correlation pattern. The first concerns the shape of the a-nullcline in the phase plane. Figure 1.4A shows that a perturbation which transiently changes the activity level can induce a phase transition if it brings the activity across threshold (the middle branch of the S-curve). Because the nullcline is much flatter on the bottom than on the top, it is easier to induce an on transition (at the sharp low knee (LK) of the S-curve) than an off transition (at the round HK). Thus, positive perturbations will be able to induce on transitions for a much larger range of s values than the range of values for which negative perturbations of the same amplitude can induce off transitions.

This effect, however, contributes only a small fraction of the variability induced by noise, because noise does not just act to create a series of quick perturbations in the activity level. The effects of noise are integrated over

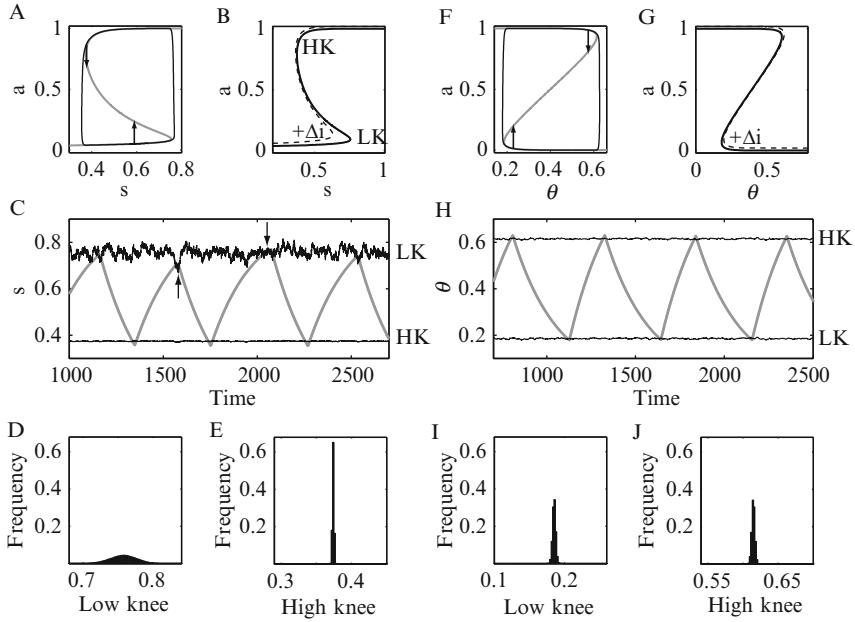

Figure 1.4 Qualitative explanation for the differences in the variability at the on and off transitions. (A) The a-nullcline and superimposed trajectory of the relaxation oscillation for the s-model. Vertical arrows show a perturbation of amplitude 0.2 that can induce a premature transition. The on transition can occur further away from the knee than the off transition. (B) The effect of a change in external input, $\Delta i = 0.01$, on the a-nullcline. (C) Time courses of the low knee (LK), high knee (HK) and s (gray, magnified from Fig. 1.3A). The upward arrow indicates a premature on transition due to noise moving the LK to a small s value. The downward arrow indicates a late on transition due to the LK maintaining its position. (D) Wide distribution of LK and (E) narrow distribution of HK obtained during the simulation. Compare with Fig. 1.3D and E. (F) Symmetrical a-nullcline and superimposed oscillation trajectory for the θ-model, with vertical arrows depicting perturbations that can induce a transition. (G) Changes in input affect the LK and HK similarly. (H) Time courses of LK, HK, and θ (gray, magnified from Fig. 1.3F). (I) Distribution of LK and (J) distribution of HK; compare with Fig. 1.3I and J.

time since noise is included in the activity equation (Eq. 1.4). Thus, if we see noise as a rapidly varying external input to the system, we also realize that it affects the a-nullcline, perturbing it. To quantify this contribution of noise, we first consider how a change Δi to a constant input to the system affects the a-nullcline. As illustrated in Fig. 1.4B, Δi shifts the LK horizontally to a greater extent than the HK. In fact, we have shown that for a small change in external input, the ratio of the resulting changes in the position of the LK and HK, $\Delta s_{lk}/\Delta s_{hk}$, is proportional to the ratio of the activity at the HK and LK, a_{hk}/a_{lk} (Tabak *et al.*, 2009). Since activity is close to 0 at the LK, this ratio can be high, around 17.4 for the parameters used here.

The prediction from this analysis with constant input is that noise will "shake" the a-nullcline during the simulation, moving the knees horizontally. Figure 1.4C shows the resulting time course of both LK and HK positions. LK varies much more than HK, as predicted, and the ratio of their standard deviations is close to 17.4. This panel also shows the time course of s (magnified from Fig. 1.3A), which increases during the silent phase and decreases during the active phase. When LK moves downward, s can cross over (upward arrow) and produce an on transition at an unusually low value of s. On the other hand, when LK remains high it can delay a transition (downward arrow). Thus, the large variations in the positions of the LK create the variability of s at the on transition. On the other hand, there is little variability of HK and therefore little variability of s at the off transition. Therefore, the wide and narrow distributions of LK (Fig. 1.4D) and HK (Fig. 1.4E) explain the wide and narrow distributions of s at the on (Fig. 1.3D) and off transitions (Fig. 1.3E).

These differences between LK and HK are absent in the θ-model. First, Fig. 1.4F shows that for subtractive negative feedback, the knees of the a-nullcline are symmetrical and therefore it is equally easy for a perturbation to induce an on or off transition (compare with Fig. 1.4A). Second, input variation affects both knees' position similarly (Fig. 1.4G). Thus, noise creates equal variations in the LK and HK (Fig 1.4H), and the variability of θ is similar at the on and off transitions. The distributions of HK and LK (Fig. 1.4I and J) are comparable to the distributions of θ at the on and off transitions (Fig. 1.3I and J).

In these examples, we used a smooth sigmoid function for a_∞, the steady-state activation of the system (Fig. 1.1). If instead, a_∞ had an abrupt onset and smooth saturation, then the Z-shaped nullcline of Fig. 1.4F would have a sharper LK, and the same pattern of correlation as the s-model could be observed. On the other hand, if the activation function was steep at higher a and smooth at lower a then the opposite correlation pattern could be observed (i.e., correlation between length of active and following—but not preceding—silent phase). Thus, the correlation pattern obtained from the θ-model depends on the exact shape of the activation function.

In contrast, for the s-model we obtain the correlation pattern shown on Fig. 1.3B and C regardless of the shape of a_∞ because the large noise-induced variations of the LK are dominant. One exception would be when θ_0 is very large, in which case the deterministic system would exhibit a stable equilibrium rather than a relaxation oscillation. That is, the oscillation is driven entirely by the noise. In this case, there should be no correlations between the active and either the preceding or the following silent phases. With this exception, the correlation pattern produced by the s-model is *very robust* to parameter changes.

In many systems, the active phase is not steady but oscillatory—this defines bursting. The slow negative feedback variable controls the transitions between active and silent phases of bursting as described above for the relaxation oscillations. However, the fast oscillations that occur during the active phase of bursting can greatly increase the sensitivity of the off transition to noise. This, in turn, can change the correlation pattern. In the following examples, we present several cases of bursting oscillations in excitable cells that exhibit different correlation patterns.

4. Example 2: Square Wave Bursting

Square wave bursting has been described in a number of cell types (Butera *et al.*, 1999; Chay and Keizer, 1983; Cornelisse *et al.*, 2001) and belongs to the class of integrator-like neurons (Izhikevich, 2001). It has two primary characteristics. One is that the spikes often ride on a depolarized plateau, as in Fig. 1.5A. However, this is not always the case, since the spikes may undershoot the plateau (Bertram *et al.*, 1995). The second characteristic is that the time between spikes progressively increases during the active phase of a burst. To investigate the correlation pattern on square wave bursting, we use a simplified version of a biophysically derived pancreatic β-cell model (Sherman and Rinzel, 1992). Equations for this and other bursting models used herein can be found in the primary references. Parameter values used were those described therein. Additionally, equations, parameter values, and computer programs for all models are available at http://www.math.fsu.edu/~bertram/software/neuron.

For the bursting models discussed, the primary observable variable is the membrane potential or voltage (V), which evolves in time according to

$$C\frac{\mathrm{d}V}{\mathrm{d}t} = -\sum\nolimits_i I_i + I_{\mathrm{noise}}. \tag{1.6}$$

The ionic currents, I_i, vary from model to model, as do the number and identity of other variables. Random noise is introduced through the term $I_{\mathrm{noise}} = m\eta$ where, η is a normally distributed random variable and m is the noise magnitude. In addition to this voltage equation, there are equations for current activation and inactivation variables. One of these variables changes slowly compared with V, and for each model is similar to θ discussed earlier, providing subtractive negative feedback.

Figure 1.5A shows the voltage time course of the model with added noise of magnitude 1 pA with the corresponding slow variable, s, superimposed. This is a slow negative feedback variable that activates an inhibitory current. When s is sufficiently large the voltage cannot reach the spike

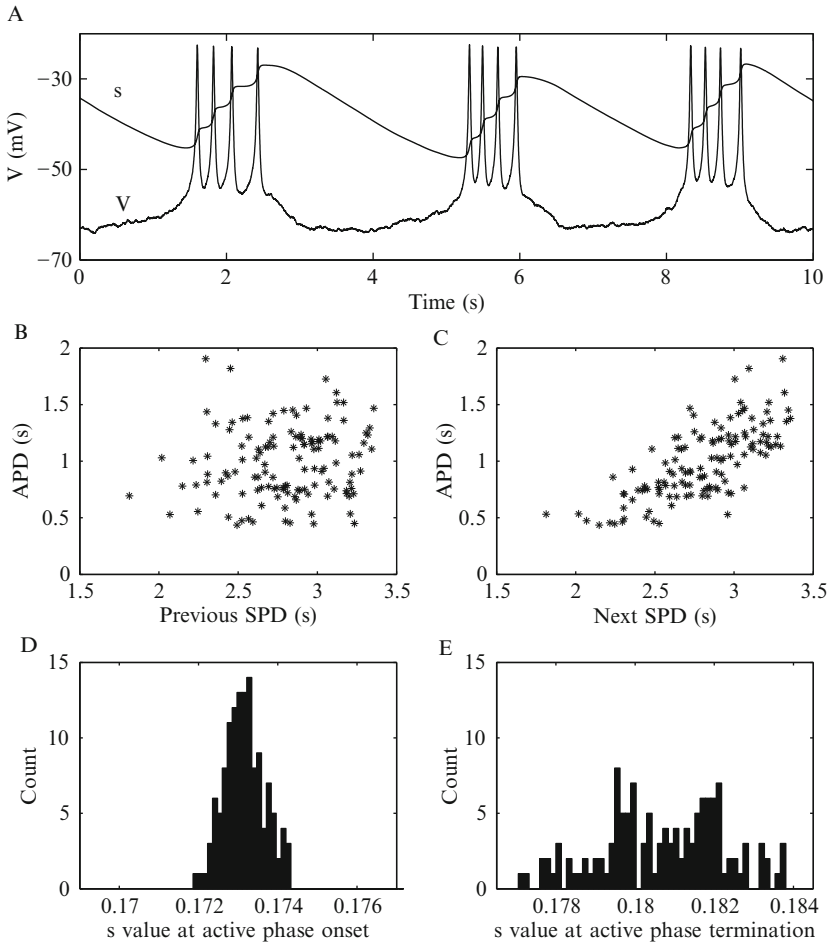

Figure 1.5 (A) Voltage trace and slow variable of a noisy square wave burster (Sherman and Rinzel, 1992). To facilitate superposition, the slow variable (s) time course has been rescaled. (B) Scatter plot obtained by plotting the duration of each active phase with the duration of the preceding silent phase. In this case, no correlation is observed ($r = 0.12$, $p = 0.15$). (C) The plot of active phase duration versus duration of the next silent phase shows a positive correlation ($r = 0.72$, $p < 10^{-20}$). Thus, on average, a short (long) active phase will be followed by a short (long) silent phase. (D) Distribution of the slow variable at the beginning of an active phase. (E) Distribution of the slow variable at the end of an active phase. The width of the slow variable distribution is greater at the active phase termination than at the active phase onset. That is, active phase termination is more sensitive to noise than active phase initiation.

threshold, so spiking stops and the cell enters a silent phase. In the absence of spiking the inhibitory s variable declines, eventually reaching a level that is low enough to allow spiking to resume.

Scatter plots of the active phase duration versus the previous and the next silent phase durations are constructed as described in the previous section. The scatter plot of the active phase versus the following silent phase (Fig. 1.5C) shows a positive correlation, indicating that short (long) active phases lead to short (long) silent phases. In panel B, however, there is no correlation between the durations of the active phase and the previous silent phase. That is, the length of the silent phase does not provide information regarding the duration of the next active phase of bursting.

To explain the correlation pattern, we plot the distributions of the values of the slow variable at the beginning and the end of an active phase. Variation of this slow variable is responsible for starting and stopping the spiking during a burst. For square wave bursting the width of the slow variable distribution is greater at the active phase termination (Fig. 1.5E) than at the active phase onset (Fig. 1.5D). The reason for this is that the spiking slows down near the end of the active phase, and the voltage spends most of its time near the spike threshold (i.e., the trajectory is approaching a homoclinic orbit), and so is sensitive to small perturbations. Thus, the termination of the burst is more subject to noise than its initiation.

This example illustrates that correlation analysis of the active and silent phase durations, when applied to a model of square wave bursting, produces a pattern with positive correlation for active versus next silent phase duration, but no correlation for active versus previous silent phase duration. This result holds for the other three models of square wave bursting tested, and the rational for this is that all models of square wave bursting have similar dynamic structures. This correlation analysis technique can be used on actual voltage data from a nerve or endocrine cell, for example, to determine if the cell is a square wave burster. It would only require that active and silent phase durations be determined and plotted as in Fig. 1.5B and C. If the patterns match those of a square wave burster, then this tells the modeler a great deal about the form that the model should take. That is, it greatly limits the range of possible models that describes the cell's electrical behavior.

5. Example 3: Elliptic Bursting

Next, we consider elliptic bursting, which is observed in several types of neurons (Del Negro *et al.*, 1998; Destexhe *et al.*, 1993; Llinas *et al.*, 1991) and belongs to the class of resonator-like neurons (Izhikevich, 2000; Llinas, 1988). Elliptic bursting is characterized by large spikes that do not ride on a depolarized plateau and small subthreshold oscillations that are present immediately before and after the active phase of a burst (Fig. 1.6A). The large spikes alone, however, do not uniquely identify this burst type, since

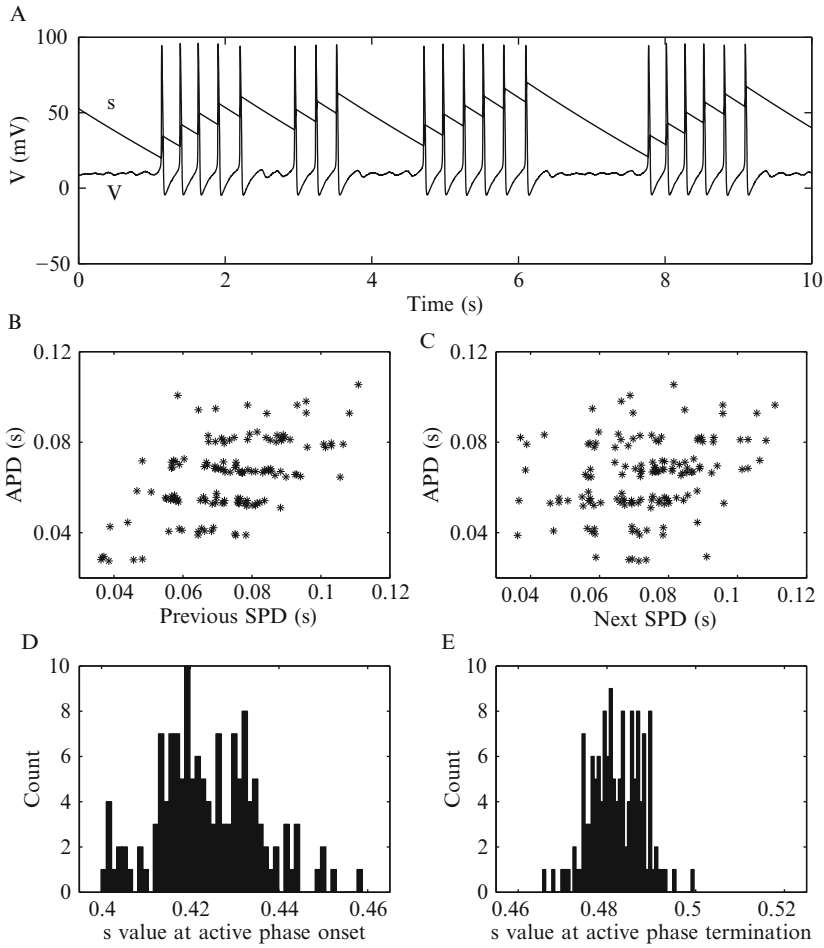

Figure 1.6 (A) Voltage trace and slow variable of an elliptic burster with noise (magnitude 0.2 pA). (B) Scatter plots of active phase duration against the duration of the previous silent phase. A correlation exists ($r = 0.53$, $p < 10^{-10}$). (C) There is a weak correlation between the durations of active phases and the following silent phases ($r = 0.22$, $p = 0.006$). (D) The width of the slow variable distribution at episode onset is greater than the distribution at active phase termination (E), thus active phase termination is less sensitive to noise than active phase initiation.

square wave bursters can have large spikes (Bertram *et al.*, 1995), as can type two or parabolic bursters (Rinzel and Lee, 1987) and other burst types. Moreover, the small subthreshold oscillations are largely obscured when noise is added to the system. That is, the subthreshold oscillations present in the deterministic system may not readily be distinguished from those introduced by the random noise. We use the reduced version of the

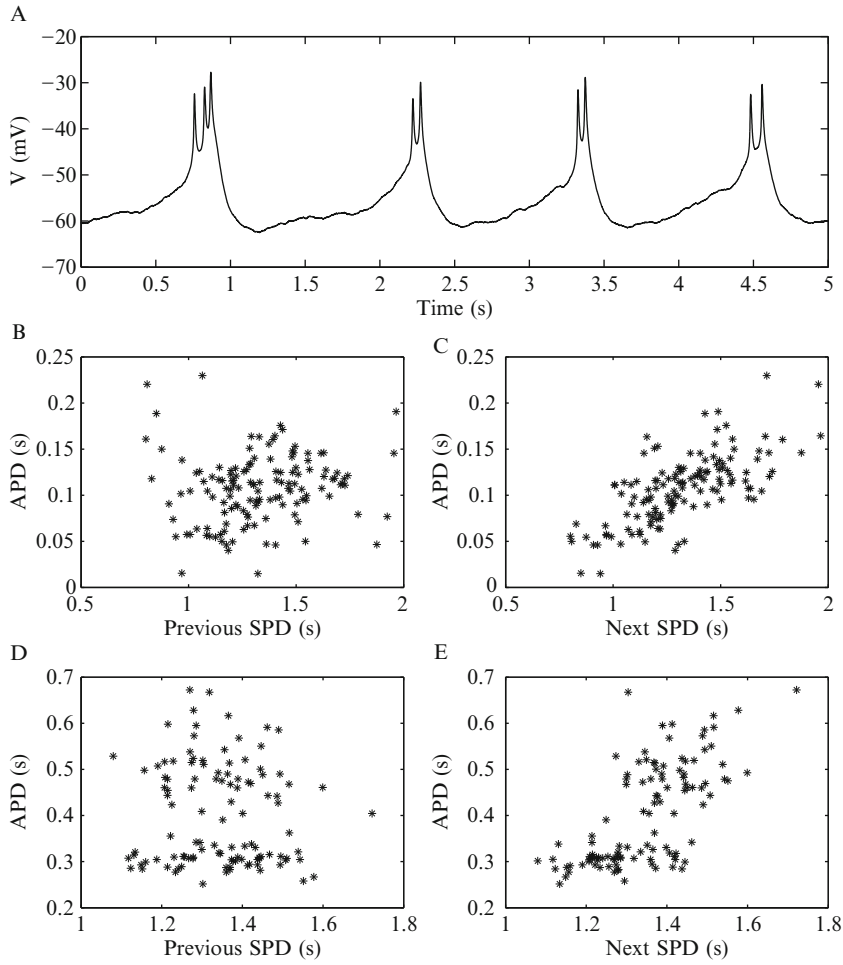

Figure 1.7 Correlation analysis applied to experimental data, and compared with a corresponding model. (A) Sample voltage trace of GH4 cell bursting. (B) Scatter plot obtained using GH4 cell data showing the active phase duration versus previous silent phase duration ($r = 0.10$, $p = 0.21$). (C) Scatter plot of active phase duration versus next silent phase duration ($r = 0.68$, $p < 10^{-20}$). (D)–(E) Scatter plots obtained from computer simulations of a model of the pituitary lactotroph (Tabak *et al.*, 2007) with noise added (4 pA magnitude), ((D), $r = -0.07$, $p = 0.43$) and ((E), $r = 0.67$, $p < 10^{-15}$).

Hodgkin–Huxley giant squid axon model (Rinzel, 1985), with an added slow outward current, to analyze the correlation patterns for elliptic bursting. Figure 1.7A shows the voltage time course of the model with noise magnitude of 0.2 pA with the corresponding slow variable superimposed.

The scatter plot of the active phase versus the duration of the previous silent phase (Fig. 1.6B) shows a positive correlation, indicating that short (long) active phase durations are preceded by short (long) silent phase durations. In contrast, there is only a weak correlation between the active phase duration and the duration of the next silent phase (Fig. 1.6C). Therefore, the duration of the previous silent phase predicts the active phase duration, but the active phase duration does not accurately predict the next silent phase duration.

As in the previous sections, we plot the distributions of the slow variable at the onset and at the termination of an active phase. The slow variable in elliptic bursting exhibits a wider distribution at burst onset (Fig. 1.6D) than at burst termination (Fig. 1.6E). The reason for the wide onset distribution is that the subthreshold oscillations bring the voltage near the spike threshold, and once this threshold is crossed an active phase is initiated. Thus, the active phase initiation is very sensitive to noise, has been described previously for this type of bursting (Kuske and Baer, 2002; Su *et al.*, 2004). During the active phase only a precise voltage perturbation at the right time can lead to spike termination (Rowat, 2007). Thus, active phase termination is relatively insensitive to the effects of noise.

This example demonstrates that application of correlation analysis can distinguish model elliptic bursting from model square wave bursting. The analysis could also be applied experimentally, taking advantage of the noise that is inherent in the system. The outcome of the analysis could help with the choice of model used to describe the biological system.

6. Example 4: Using Correlation Analysis on Experimental Data

In this example, we illustrate how correlation analysis can be used as a test for the validity of a model by applying it to both the model and the experimental system. The model describes fast bursting electrical activity in prolactin-secreting pituitary lactotrophs (Tabak *et al.*, 2007). The experimental preparation is the GH4 pituitary lactotroph cell line. Like primary lactotrophs, cells from this lactotroph cell line often exhibit fast bursting electrical oscillations. A sample trace of GH4 bursting activity is shown in Fig. 1.7A. Correlation analysis was applied to a voltage trace approximately 5-min long, consisting of $\sim$150 bursts. The scatter plots show that there is no correlation between active phase duration and the previous silent phase (Fig. 1.7B), but a strong positive correlation between active phase duration and the next silent phase duration (Fig. 1.7C).

We next compare these scatter plots with those from computer simulations of the model with added noise of magnitude 4 pA. The bursting

produced by the model is neither square wave nor elliptic (Tabak *et al.*, 2007), but instead is of the type referred to as pseudo-plateau (Stern *et al.*, 2008). The model scatter plots show that, as with the experimental data, there is no correlation between active and previous silent phase durations (Fig. 1.7D), and a strong positive correlation between the active and the next silent phase durations (Fig. 1.7E). Thus, the correlation analysis provides some support for the validity of the mechanism for bursting in the mathematical model.

7. Summary

We have demonstrated that correlation analysis can be a useful tool for comparing mathematical models with experimental data as a first check for the validity of the model. This type of analysis is appropriate for systems that produce relaxation oscillations or bursting oscillations. While it does not validate the model, it is a first test that is simple to apply to both the model and the biological system. Furthermore, it is noninvasive: all that is required is that one measure the activity of the biological system and make scatter plots of active and silent phase durations. Because the correlation analysis is a statistical test, confidence in the results increases with the number of data points. In this case, the data points are bursts or relaxation oscillations. For our example with the GH4 lactotroph cell line, 5 min of continuous recording was sufficient to give reliable results. While our examples focused on neural oscillations, the method is equally applicable to other types of biological systems that generate relaxation-type oscillations.

Appendix: Algorithm for the Determination of Phase Durations During Bursting

Here, we describe the method used to determine silent and active phase durations for a noisy burst time course, where V is the observable. Upon visual inspection, we first set a threshold, V_S, such that if $V > V_S$ a spike is recorded. Denote the times at which two spikes occur by t_i and t_j, then two spikes are considered to lie within a single burst if $|t_i - t_j| < \delta$, where, δ is a positive parameter chosen by examination of interspike intervals. Conversely, if $|t_i - t_j| > \delta$ then the two spikes are not considered part of the same burst. In a similar way, we obtain the duration of each silent phase by computing the difference between the last spike of a burst and the first spike of the following burst. We then create three vectors of equal size. One vector, $\overrightarrow{b}$, contains all the active phase durations in chronological order (i.e., $[b_1, b_2, \ldots, b_N]$). The other two vectors contain the silent phase durations.

The preceding silent phase vector is $\overrightarrow{s_{\text{prec}}} = [s_1, s_2, ..., s_N]$, while the following silent phase vector is $\overrightarrow{s_{\text{next}}} = [s_2, s_3, ..., s_{N+1}]$. We then plot the elements of $\overrightarrow{b}$ versus those of $\overrightarrow{s_{\text{prec}}}$ or versus $\overrightarrow{s_{\text{next}}}$ to make scatter plots. Computer codes for the computation of active and silent phase durations can be downloaded from http://www.math.fsu.edu/~bertram/software/neuron.

In the case of experimental data, the data may have to be detrended if any slow trends in active and silent phase durations are present.

ACKNOWLEDGMENT

This work was supported by NIH grant DA-19356.

REFERENCES

Bertram, R., and Sherman, A. (2005). Negative calcium feedback: The road from Chay-Keizer. *In* "Bursting: The Genesis of Rhythm in the Nervous System," (S. Coombes and P. C. Bressloff, eds.), World Scientific, Singapore.

Bertram, R., Butte, M., Kiemel, T., and Sherman, A. (1995). Topological and phenomenological classification of bursting oscillations. *Bull. Math. Biol.* **57,** 413–439.

Butera, R. J., Rinzel, J., and Smith, J. C. (1999). Models of respiratory rhythm generation in the pre-Bötzinger complex I. Bursting pacemaker neurons. *J. Neurophysiol.* **82,** 382–397.

Chay, T. R., and Keizer, J. (1983). Minimal model for membrane oscillations in the pancreatic β-cell. *Biophys. J.* **42,** 181–190.

Coombes, S., and Bressloff, P.C (2005). Bursting: The Genesis of Rhythm in the Nervous System. World Scientific Publishing Co., Singapore.

Cornelisse, L. N., Scheenen, W. J. J. M., Koopman, W. J. H., Roubos, E. W., and Gielen, S. C. A. M. (2001). Minimal model for intracellular calcium oscillations and electrical bursting in melanotrope cells of *Xenopus laevis*. *Neural Comput.* **13,** 113–137.

Dean, P. M., and Mathews, E. K. (1970). Glucose-induced electrical activity in pancreatic islet cells. *J. Physiol.* **210,** 255–264.

Del Negro, C. A., Hsiao, C.-F., Chandler, S. H., and Garfinkel, A. (1998). Evidence for a novel bursting mechanism in rodent trigeminal neurons. *Biophys. J.* **75,** 174–182.

Destexhe, A., Babloyantz, A., and Sejnowski, T. J. (1993). Ionic mechanisms for intrinsic slow oscillations in thalamic relay neurons. *Biophys. J.* **65,** 1538–1552.

Ermentrout, G. B., and Chow, C. C. (2002). Modeling neural oscillations. *Physiol. Behav.* **77,** 629–633.

Friesen, W. O., and Block, G. D. (1984). What is a biological oscillator? *Am. J. Physiol.* **246,** R847–R853.

Goldbeter, A., and Lefever, R. (1972). Dissipative structures for an allosteric model; application to glycolytic oscillations. *Biophys. J.* **12,** 1302–1315.

Izhikevich, E. M. (2000). Neural excitability, spiking and bursting. *Int. J. Bifur. Chaos.* **10,** 1171–1266.

Izhikevich, E. M. (2001). Resonate-and-fire neurons. *Neural Netw.* **14,** 883–894.

Kuske, R., and Baer, S. M. (2002). Asymptotic analysis of noise sensitivity in a neuronal burster. *Bull. Math. Biol.* **64,** 447–481.

Li, Y.-X., Stojilkovic, S. S., Keizer, J., and Rinzel, J. (1997). Sensing and refilling calcium stores in an excitable cell. *Biophys. J.* **72,** 1080–1091.

Lim, S., and Rinzel, J. Noise-induced transitions in slow wave neuronal dynamics. *J. Comput. Neurosci.* (in press).

Llinas, R. R. (1988). The intrinsic electrophysiological properties of mammalian neurons: Insights into central nervous system function. *Science* **242,** 1654–1664.

Llinas, R. R., Grace, T., and Yarom, Y. (1991). *In vitro* neurons in mammalian cortical layer 4 exhibit intrinsic oscillatory activity in the 10- to 50-Hz frequency range. *Proc. Natl. Acad. Sci. USA* **88,** 897–901.

Murray, J. D. (1989). Mathematical Biology. Springer-Verlag, Berlin.

Rinzel, J. (1985). Excitation dynamics: Insights from simplified membrane models. *Fed. Proc.* **44,** 2944–2946.

Rinzel, J. (1987). A formal classification of bursting mechanisms in excitable systems. *In* "Mathematical Topics in Population Biology, Morphogenesis and Neurosciences," (E. Teramoto and M. Yamaguti, eds.), Vol. 71. Springer-Verlag, Berlin.

Rinzel, J., and Ermentrout, G. B. (1998). Analysis of neural excitability and oscillations. *In* "Methods in Neuronal Modeling: From Ions to Networks," (C. Koch and I. Segev, eds.), pp. 251–291. MIT Press, Cambridge.

Rinzel, J., and Lee, Y. S. (1987). Dissection of a model for neuronal parabolic bursting. *J. Math. Biol.* **25,** 653–675.

Rowat, P. (2007). Interspike interval statistics in the stochastic Hodgkin–Huxley model: Coexistence of gamma frequency bursts and highly irregular firing. *Neural Comput.* **19,** 1215–1250.

Sherman, A., and Rinzel, J. (1992). Rhythmogenic effects of weak electrotonic coupling in neuronal models. *Proc. Natl. Acad. Sci. USA* **89,** 2471–2474.

Shpiro, A., Curtu, R., Rinzel, J., and Rubin, N. (2007). Dynamical characteristics common to neuronal competition models. *J. Neurophysiol.* **97,** 462–473.

Stern, J. V., Osinga, H. M., LeBeau, A., and Sherman, A. (2008). Resetting behavior in a model of bursting in secretory pituitary cells: Distinguishing plateaus from pseudo-plateaus. *Bull. Math. Biol.* **70,** 68–88.

Strogatz, S. H. (1994). Nonlinear dynamics and chaos. Addison-Wesley, Reading, MA.

Su, J., Rubin, J., and Terman, D. (2004). Effects of noise on elliptic bursters. *Nonlinearity* **17,** 1–25.

Tabak, J., Rinzel, J., and O'Donovan, M. J. (2001). The role of activity-dependent network depression in the expression and self-regulation of spontaneous activity in the developing spinal cord. *J. Neurosci.* **21,** 8966–8978.

Tabak, J., O'Donavan, M. J., and Rinzel, J. (2006). Differential control of active and silent phases in relaxation models of neuronal rhythms. *J. Comput. Neurosci.* **21,** 307–328.

Tabak, J., Toporikova, N., Freeman, M. E., and Bertram, R. (2007). Low dose of dopamine may stimulate prolactin secretion by increasing fast potassium currents. *J. Comput. Neurosci.* **22,** 211–222.

Tabak, J., Senn, W., O'Donovan, M. J., and Rinzel, J. (2000). Modeling of spontaneous activity in developing spinal cord using activity-dependent depression in an excitatory network. *J. Neurosci.* **20,** 3041–3056.

Tabak, J., Mascagni, M., and Bertram, R. (2009). *Mechanism for the universal pattern of activity in developing neuronal networks, submitted.*

Tsai, T. Y.-C., Choi, Y. S., Ma, W., Pomerening, J. R., Tang, C., and Ferrell, J. E. Jr. (2008). Robust, tunable biological oscillations from interlinked positive and negative feedback loops. *Science* **321,** 126–129.

Tsaneva-Atanasova, K., Sherman, A., Van Goor, F., and Stojilkovic, S. S. (2007). Mechanism of spontaneous and receptor-controlled electrical activity in pituitary somatotrophs: Experiments and theory. *J. Neurophysiol.* **98,** 131–144.

Tyson, J. J. (1991). Modeling the cell division cycle: cdc2 and cyclin interactions. *Proc. Natl. Acad. Sci. USA* **88,** 7328–7332.

van der Pol, B., and van der Mark, J. (1928). The heartbeat considered as a relaxation oscillation, and an electrical model of the heart. *Phil. Mag.* **6,** 763–775.

Van Goor, F., Zivadinovic, D., Martinez-Fuentes, A. J., and Stojilkovic, S. S. (2001). Dependence of pituitary hormone secretion on the pattern of spontaneous voltage-gated calcium influx. *J. Biol. Chem.* **276,** 33840–33846.

Wilson, H. R., and Cowan, J. D. (1972). Excitatory and inhibitory interactions in localized populations of model neurons. *Biophys. J.* **12,** 1–24.